ORIGINAL ARTICLE

Cancer Science WILEY

Antitumor activity of α-pinene in T-cell tumors

Masaya Abe[1] | Noboru Asada[2] | Maiko Kimura[1] | Chie Fukui[3] | Daisuke Yamada[4] |
Ziyi Wang[5] | Masayuki Miyake[6] | Takeshi Takarada[4] | Mitsuaki Ono[5] |
Michinori Aoe[6] | Wataru Kitamura[1] | Masayuki Matsuda[1] | Takashi Moriyama[1] |
Akifumi Matsumura[1] | Yoshinobu Maeda[1]

[1]Department of Hematology, Oncology and Respiratory Medicine, Okayama University Graduate School of Medicine, Dentistry and Pharmaceutical Sciences, Okayama, Japan

[2]Department of Hematology and Oncology, Okayama University Hospital, Okayama, Japan

[3]Division of Hematology, Department of Medicine, Kobe University Hospital, Kobe, Japan

[4]Department of Regenerative Science, Okayama University Graduate School of Medicine, Dentistry and Pharmaceutical Sciences, Okayama, Japan

[5]Department of Molecular Biology and Biochemistry, Okayama University Graduate School of Medicine, Dentistry and Pharmaceutical Sciences, Okayama, Japan

[6]Division of Medical Support, Okayama University Hospital, Okayama, Japan

Correspondence
Noboru Asada, Department of Hematology and Oncology, Okayama University Hospital, 2-5-1 Shikata-cho, Kita-Ku, Okayama 700-8558, Japan.
Email: nasada@okayama-u.ac.jp

Funding information
Teraoka Scholarship Foundation; Wesco Scientific Promotion Foundation

Abstract

T-cell acute leukemia and lymphoma have a poor prognosis. Although new therapeutic agents have been developed, their therapeutic effects are suboptimal. α-Pinene, a monoterpene compound, has an antitumor effect on solid tumors; however, few comprehensive investigations have been conducted on its impact on hematologic malignancies. This report provides a comprehensive analysis of the potential benefits of using α-pinene as an antitumor agent for the treatment of T-cell tumors. We found that α-pinene inhibited the proliferation of hematologic malignancies, especially in T-cell tumor cell lines EL-4 and Molt-4, induced mitochondrial dysfunction and reactive oxygen species accumulation, and inhibited NF-κB p65 translocation into the nucleus, leading to robust apoptosis in EL-4 cells. Collectively, these findings suggest that α-pinene has potential as a therapeutic agent for T-cell malignancies, and further investigation is warranted.

KEYWORDS
alpha-pinene, apoptosis, hematologic malignancies, lymphoblastic leukemia, acute, T-cell, T-cell lymphoma

1 | INTRODUCTION

Hematologic malignancies are highly heterogeneous diseases that are classified into more than 100 types according to the WHO classification.[1] Among hematologic malignancies, T-ALL and T-cell malignant lymphoma (T-lymphoma) are aggressive, often resistant to treatment, and prone to early recurrence.[2,3] T-ALL accounts for 10%–15% of cases of pediatric ALL and up to 25% of cases of adult ALL. Overall survival is 80% in children, but less than 50% due to high treatment-related toxicity in adults.[4] Therefore, novel therapies are needed for T-ALL and T-lymphoma.

Plant-derived essential oils have antibacterial, antifungal, antiviral, anti-inflammatory, and antitumor effects.[5] α-Pinene, an aromatic monoterpene, is a component of essential oils. α-Pinene suppresses tumor growth in colon cancer cells.[6] The mechanism of the antitumor effect of α-pinene in malignant melanoma was the induction of apoptosis evidenced by early disruption of mitochondrial membrane potential (MMP), ROS production, increase in caspase-3 activity, heterochromatin aggregation, DNA fragmentation and exposure of phosphatidyl serine, and reduced tumor metastasis to the lungs in mice.[7] α-Pinene also inhibits tumor growth in human prostate cancer cells by inducing apoptosis and cell-cycle arrest.[8] In this study, immunohistochemistry in tumor tissues revealed the reduction of Ki-67 and proliferation cell nuclear antigen, and the increase in TUNEL-positive cells. Furthermore, α-pinene did not show any toxicity in major organs, including the heart, liver, intestine, kidney and spleen.[8] Kusuhara et al. showed that administration of α-pinene by inhalation elicits a tumor-suppressing effect in a mouse model of malignant melanoma.[9] Moreover, intriguingly, inhalation of α-pinene may activate an antitumor immune response, as indicated by an increase in B-cells, T-cells, and natural killer (NK) cells.[10] Another study suggested that α-pinene enhances anticancer activity by accelerating NK-cell activation and cytotoxicity via the ERK/AKT signaling pathway.[11] α-Pinene thus has potential as an antitumor agent. In this study, we investigated the effect of α-pinene on cell growth in hematologic malignancies, especially in T-cell tumors in vitro and in vivo.

2 | MATERIALS AND METHODS

2.1 | Chemicals and reagents

α-Pinene, (R)-(+)-limonene (limonene), DMSO, PMA, and ionomycin were purchased from Sigma-Aldrich (St. Louis, MO, USA). NAC and 4% PFA were purchased from Fujifilm Wako Pure Chemical Corporation (Osaka, Japan). α-Pinene, limonene, PMA, and ionomycin were dissolved in DMSO. The final concentration of DMSO was <0.5 v/v%. Control groups were treated with a medium containing <0.5 v/v% DMSO.

2.2 | Cell lines

Murine T-lymphoma cell line EL-4, murine multiple myeloma cell line 5TGM1-Luc, human T-ALL cell lines Molt-4, CCRF-CEM and HPB-ALL, human acute myeloid leukemia cell lines KG-1a and HNT-34, human chronic myelogenous leukemia cell line K562, and human B-ALL cell lines BALM-7 and NALM-6 were cultured in RPMI 1640 with 10% fetal bovine serum (Thermo Fisher Scientific, Waltham, MA, USA). Human acute promyelocytic leukemia cell line HL-60 was cultured in RPMI 1640 with 20% fetal bovine serum. All the cell lines were incubated at 37°C in 5% CO_2.

2.3 | Cell growth inhibition assay, cell-cycle analysis, and apoptosis assay

Cell Counting Kit-8 (CCK-8; Dojindo Laboratories, Kumamoto, Japan) was used to test the viability of the cell lines, human blood T-cells and mouse spleen T-cells. Cells were seeded at a density of 5×10^4 cells/well in a 24-well plate and treated with α-pinene or limonene in the presence or absence of NAC at set times. Details are provided in Appendix S1.

2.4 | RNA-sequencing analysis

Cells were treated with or without α-pinene for 6h. Total RNA was extracted from treated cells using the RNeasy Mini Kit including an RNase-Free DNase Set (Qiagen, Venlo, Netherlands). The quantity and quality of the RNA were verified using a NanoDrop ND-1000 spectrophotometer (Thermo Fisher Scientific) and the 2200 TapeStation (Agilent Technologies, Santa Clara, CA, USA). RNA-seq libraries were prepared using GenomeLead (Kagawa, Japan) and sequenced as 2×150 bp paired-end reads on a DNBSEQ-G400RS analyzer (MGI, Shenzhen, China). Details are provided in Appendix S1.

2.5 | Measurement of total intracellular reactive oxygen species

DCFH-DA (Sigma-Aldrich) is converted to DCF in the presence of ROS. Total intracellular ROS levels were measured using a DCFH-DA

FIGURE 1 α-Pinene and limonene inhibited the proliferation of T-cell tumors in vitro. (A) Anti-proliferative effect of α-pinene or limonene at 36h on EL-4 and Molt-4 cells, as determined by the CCK-8 assay. (B) EL-4 cells were treated with α-pinene or limonene at the indicated concentrations and measured using the CCK-8 assay at the specified time points. (C) EL-4 cells were incubated with 50 μg/mL α-pinene or limonene for 36h and images were captured. The scale bars indicate 50 μm (20 μm in the enlarged image). (D) Apoptosis assay in EL-4 cells treated with 50 μg/mL of α-pinene or limonene at the specified time points. (E) Cell-cycle analysis of EL-4 cells treated with 10 μg/mL α-pinene or limonene at the indicative time points. All data are based on at least three independent experiments. The results are reported as the mean±SEM. (A. B) Data were compared with the control group using two-tailed independent samples t-tests. (D, E) Results were analyzed using one-way ANOVA; *$p < 0.05$, **$p < 0.01$, ***$p < 0.001$, ****$p < 0.0001$.
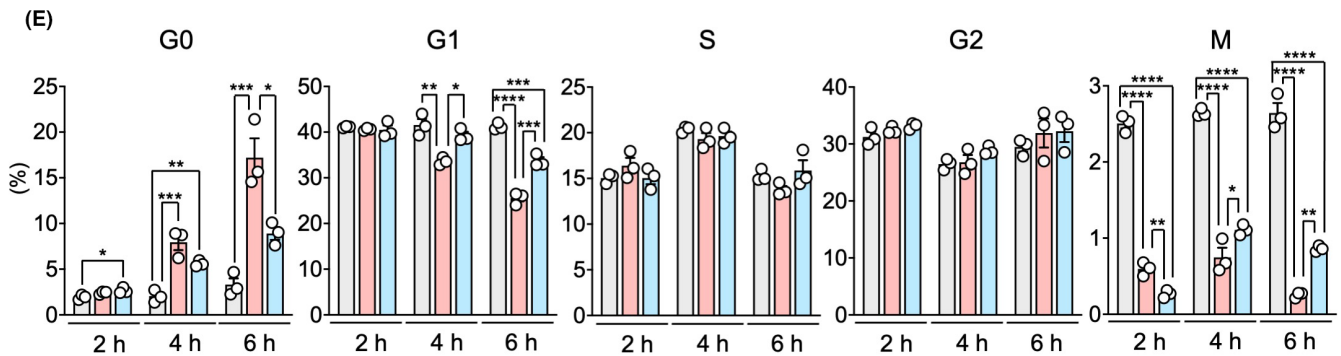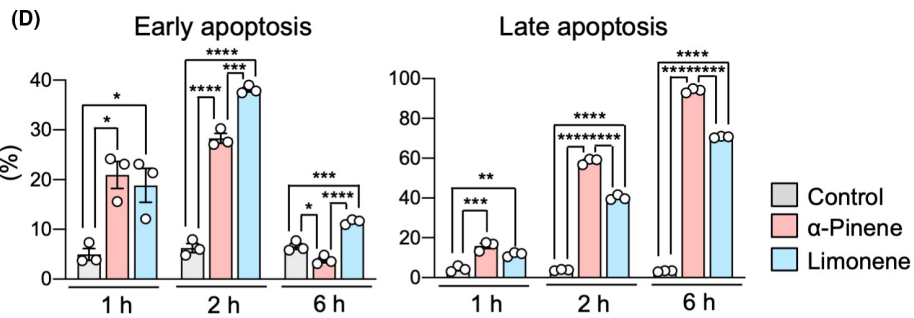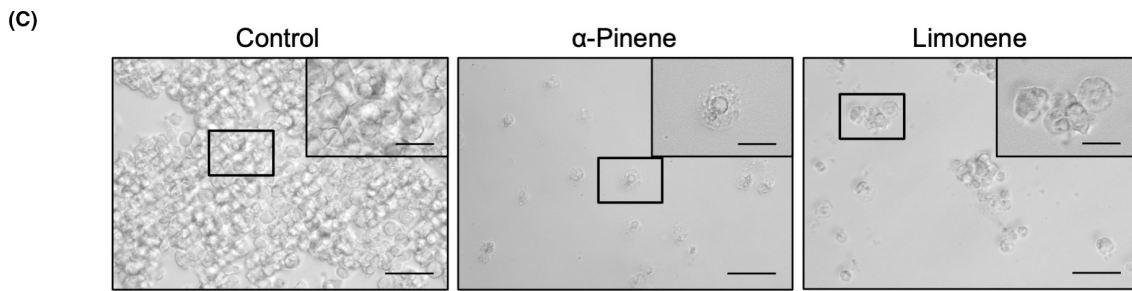
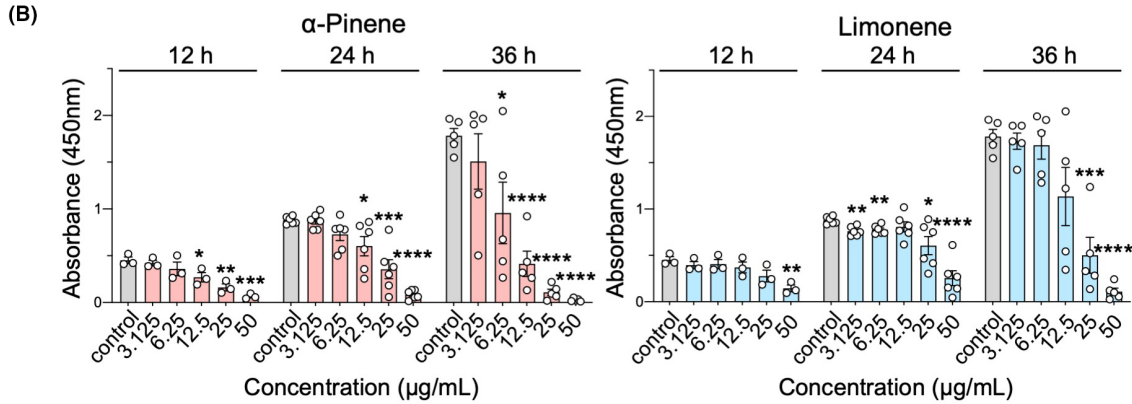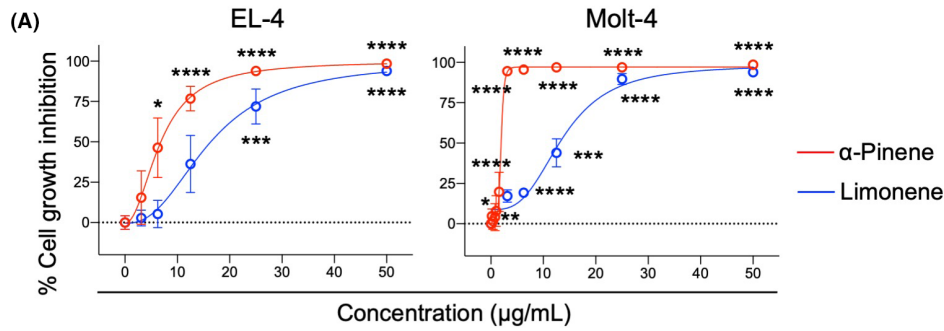**TABLE 1** IC$_{50}$ (μg/mL) values treated with α-pinene and limonene for 36 h against hematologic malignancy cell lines, human blood T-cells, and murine spleen T-cells.

Cell line	EL-4	Molt-4	CCRF-CEM	HPB-ALL	KG-1a	HNT-34	HL-60
α-Pinene (μg/mL)	6.82±1.60	1.93±0.14	2.64±0.18	1.68±0.46	2.63±0.13	3.71±0.47	n.d.
Limonene (μg/mL)	16.24±3.75	13.78±1.25	n.d.	n.d.	10.62±5.27	n.d.	n.d.
Cell line/cell	K562	BALM-7	NALM-6	5TGM1-Luc	Human blood T-cells	Murine spleen T-cells	
α-Pinene (μg/mL)	n.d.	0.46±0.04	n.d.	2.02±1.09	n.d.	n.d.	
Limonene (μg/mL)	n.d.	7.59±0.56	n.d.	5.96±0.73	n.d.	n.d.	

Note: All data are representative of at least three independent experiments. Data are represented as mean±SEM. n.d.; not detected (not possible to determine the appropriate concentration that inhibits 50% cell growth).

probe. Cells were seeded at a density of 5×10^4 cells/well in a 24-well plate and treated with α-pinene in the presence or absence of NAC for 1 h. DCFH-DA containing DAPI was added to treated cells (final DCFH-DA concentration: 10 μM), and cells were incubated for 20 min at 37°C. The ROS levels were then measured immediately using FCM.

2.6 | Quantification of DNA double-stranded breaks

Cells were seeded at a density of 5×10^4 cells/well in a 24-well plate and treated with α-pinene in the presence or absence of NAC for 6 h; fixed in 2% PFA in PBS for 5 min; washed, and permeabilized with 0.1% Triton X-100 in PBS for 5 min; and then incubated with an Alexa Fluor 647-conjugated anti-phospho-H2AX (Ser139) (γH2AX) antibody (BioLegend, 0.2:100) in PBS for 30 min. γH2AX was measured using FCM.

2.7 | Measurement of mitochondrial membrane potential

Tetramethylrhodamine ethyl ester (TMRE; Sigma-Aldrich) was used to detect MMP. Cells were seeded at a density of 5×10^4 cells/well in a 24-well plate and treated with α-pinene in the presence or absence of NAC for 24 h. The treated cells were washed and incubated with 200 nM TMRE for 20 min at 37°C. MMP was then measured immediately using FCM.

2.8 | Measurement of oxygen consumption rate

Cells were seeded at a density of 2×10^5 cells/well in a 96-well plate and treated with α-pinene. Extracellular OCR Plate Assay Kit (Dojindo Laboratories) was used to measure oxygen consumption. The fluorescence intensity (Ex: 500 nm, Em: 650 nm) was measured every 10 min for 200 min using a fluorescence microplate reader, FlexStation 3 (Molecular Devices, San Jose, CA, USA). The oxygen consumption rate (OCR) was calculated according to the manufacturer's instructions.
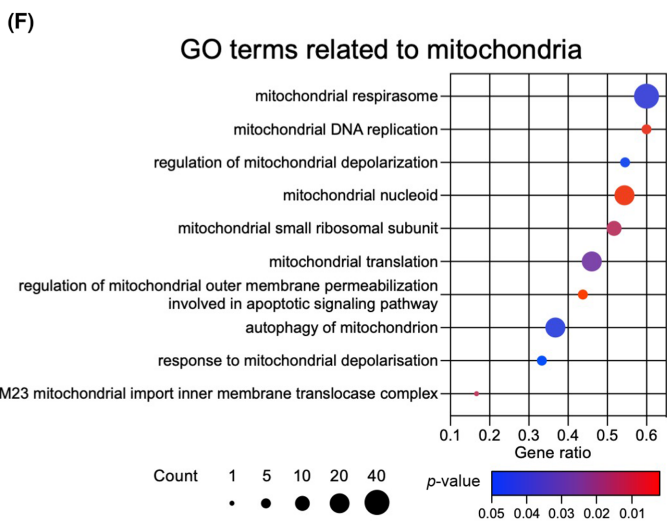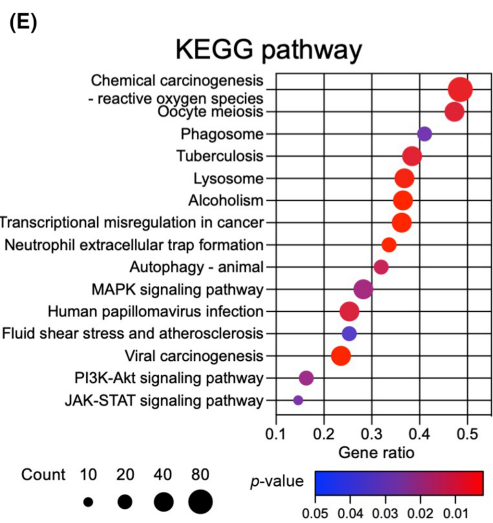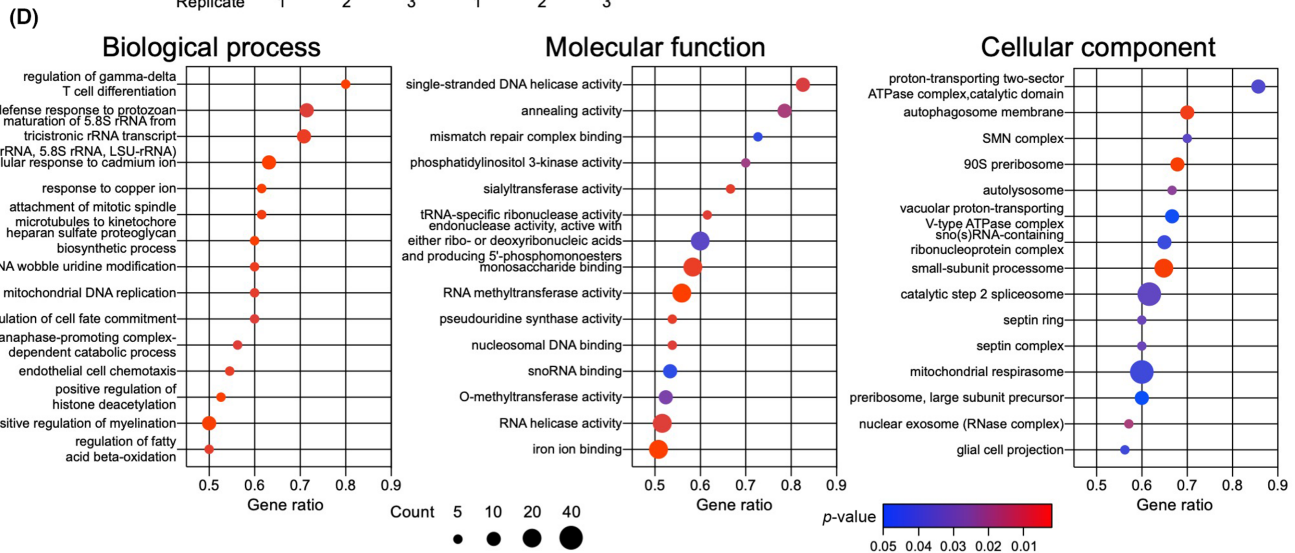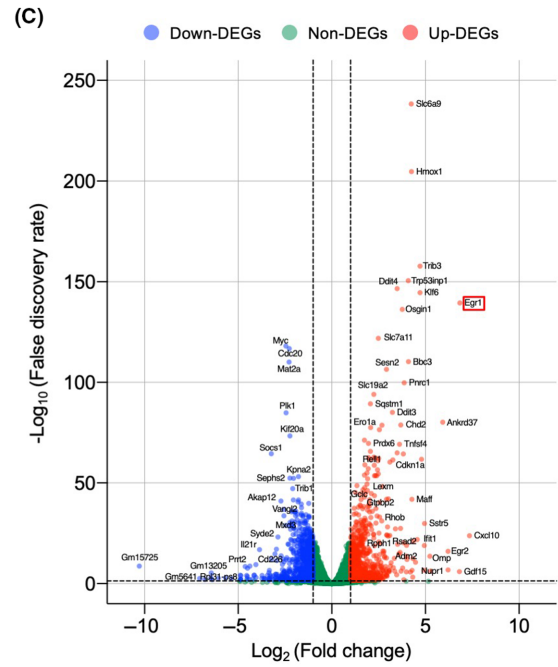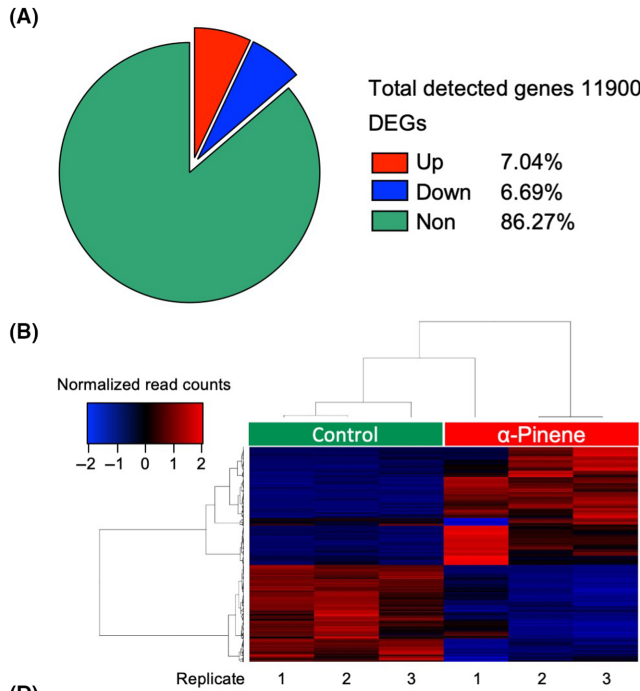
2.9 | Measurement of glucose and lactate of the cell culture supernatant

Cells were seeded at a density of 5×10^4 cells/well in a 24-well plate and treated with α-pinene for 24 h. Glucose and lactate concentrations of the cell culture supernatant were measured using a glucose and lactate assay kit (Dojindo Laboratories). DAPI⁻ live cells were counted with FCM.

2.10 | Measurement of mitochondrial superoxide

The mtSOX Deep Red (Dojindo Laboratories) was used to measure mitochondrial superoxide levels. Cells, resuspended with mtSOX Deep Red containing DAPI, were seeded at a density of 5×10^4 cells/well in a 24-well plate and treated with α-pinene in the presence or absence of NAC for 1 h (final mtSOX Deep Red concentration: 5 μM). The mitochondrial superoxide levels were measured immediately using FCM.

FIGURE 2 RNA-seq analysis of EL-4 cells treated with α-pinene. EL-4 cells were treated with or without α-pinene 10 μg/mL for 6 h. Total RNA extracted from the cells was prepared for RNA-seq libraries and the libraries sequenced with DNBSEQ-G400RS. (A) Pie chart showing the total number of genes detected and percentage of upregulated and downregulated differentially expressed genes (DEGs). (B) Heatmap of unsupervised hierarchical clustering of significantly enriched genes for EL-4 cells treated with α-pinene. Red and blue shading indicates upregulation and downregulation, respectively. (C) Volcano plot of the genes. The upregulated, downregulated and non-DEGs are shown as red, blue, and green dots, respectively. Bubble plots of gene set enrichment analysis (GSEA) using (D) Gene Ontology (GO) terms, (E) Kyoto Encyclopedia of Genes and Genomes (KEGG) pathway, and (F) GO terms related to mitochondria. All data shown are based on three control samples and three α-pinene samples. DEGs were defined as false discovery rate < 0.05 and |log$_2$ (fold change)| > 1. Significantly enriched GO and KEGG pathway in GSEA were defined as $p < 0.05$. Down-DEGs, downregulated DEGs; Non-DEGs, non-DEG genes; Up-DEGs, upregulated DEGs.

(A)

Total detected genes 11900
DEGs
Up   7.04%
Down   6.69%
Non   86.27%

(B)

Normalized read counts

−2 −1 0 1 2

Control   α-Pinene

Replicate 1 2 3   1 2 3

(C)

Down-DEGs   Non-DEGs   Up-DEGs

−Log$_{10}$ (False discovery rate)

Log$_2$ (Fold change)

(D)

Biological process

regulation of gamma-delta T cell differentiation
defense response to protozoan
maturation of 5.8S rRNA from tricistronic rRNA transcript (SSU-rRNA, 5.8S rRNA, LSU-rRNA)
cellular response to cadmium ion
response to copper ion
attachment of mitotic spindle microtubules to kinetochore
heparan sulfate proteoglycan biosynthetic process
tRNA wobble uridine modification
mitochondrial DNA replication
regulation of cell fate commitment
anaphase-promoting complex-dependent catabolic process
endothelial cell chemotaxis
positive regulation of histone deacetylation
positive regulation of myelination
regulation of fatty acid beta-oxidation

Gene ratio

Molecular function

single-stranded DNA helicase activity
annealing activity
mismatch repair complex binding
phosphatidylinositol 3-kinase activity
sialyltransferase activity
tRNA-specific ribonuclease activity endonuclease activity, active with either ribo- or deoxyribonucleic acids and producing 5'-phosphomonoesters
monosaccharide binding
RNA methyltransferase activity
pseudouridine synthase activity
nucleosomal DNA binding
snoRNA binding
O-methyltransferase activity
RNA helicase activity
iron ion binding

Gene ratio

Cellular component

proton-transporting two-sector ATPase complex, catalytic domain
autophagosome membrane
SMN complex
90S preribosome
autolysosome
vacuolar proton-transporting V-type ATPase complex
sno(s)RNA-containing ribonucleoprotein complex
small-subunit processome
catalytic step 2 spliceosome
septin ring
septin complex
mitochondrial respirasome
preribosome, large subunit precursor
nuclear exosome (RNase complex)
glial cell projection

Gene ratio

Count 5 10 20 40

p-value

0.05 0.04 0.03 0.02 0.01

(E)

KEGG pathway

Chemical carcinogenesis - reactive oxygen species
Oocyte meiosis
Phagosome
Tuberculosis
Lysosome
Alcoholism
Transcriptional misregulation in cancer
Neutrophil extracellular trap formation
Autophagy - animal
MAPK signaling pathway
Human papillomavirus infection
Fluid shear stress and atherosclerosis
Viral carcinogenesis
PI3K-Akt signaling pathway
JAK-STAT signaling pathway

Gene ratio

Count 10 20 40 80

p-value

0.05 0.04 0.03 0.02 0.01

(F)

GO terms related to mitochondria

mitochondrial respirasome
mitochondrial DNA replication
regulation of mitochondrial depolarization
mitochondrial nucleoid
mitochondrial small ribosomal subunit
mitochondrial translation
regulation of mitochondrial outer membrane permeabilization involved in apoptotic signaling pathway
autophagy of mitochondrion
response to mitochondrial depolarisation
TIM23 mitochondrial import inner membrane translocase complex

Gene ratio

Count 1 5 10 20 40

p-value

0.05 0.04 0.03 0.02 0.01

2.11 | Quantitative real-time polymerase chain reaction assay

Total RNA from treated cells was extracted using the RNeasy Mini Kit, and reverse transcription was performed using SuperScript II Reverse Transcriptase (Thermo Fisher Scientific), according to the manufacturer's protocols. Primer sequences are provided in Table S1. Details are provided in Appendix S1.

2.12 | Quantification of p53 and phosphorylated p53

EL-4 cells were seeded at a density of 5×10^4 cells/well in a 24-well plate and treated with α-pinene (10 μg/mL) for 3 h, and Molt-4 cells were treated with α-pinene (2 μg/mL) for 6 h. The staining protocol is provided in Appendix S1.

2.13 | Detection of active caspase-3

Cells were seeded at a density of 5×10^4 cells/well in a 24-well plate and treated with α-pinene in the presence or absence of NAC for 24 h; fixed in 2% PFA in PBS for 5 min; washed, and permeabilized with 0.1% Triton X-100 in PBS for 5 min; and then incubated with an anti-active caspase-3 antibody (Becton, Dickinson and Company, 2:100) in PBS for 30 min. Active caspase-3 was measured using FCM.

2.14 | Immunocytochemistry

EL-4 cells were seeded at a density of 5×10^4 cells/well in a 24-well plate; treated with 10 μg/mL α-pinene for 4 h; and then treated with 80 nM PMA and 1 μM ionomycin for 20 min. Details are provided in Appendix S1.

2.15 | Quantification of NF-κB p65

EL-4 cells were seeded at a density of 5×10^5 cells/well in a 6-well plate, treated with α-pinene (10 μg/mL) for 4 h, and treated with PMA (80 nM) and ionomycin (1 μM) for 20 min. Details are provided in Appendix S1.

2.16 | Animals

Seven-week-old female C57BL/6J mice were purchased from CLEA Japan (Tokyo, Japan). All mice were maintained under specific pathogen-free conditions and under a 12 h light/12 h dark cycle. All animal experimental procedures were approved by the Animal Care and Use Committee of Okayama University Advanced Science Research Center.

2.17 | EL-4 Luc mouse tumor model

Details of the luciferase-expressing EL-4 (EL-4 Luc) cell generation methods are provided in Appendix S1. EL-4 Luc cell suspensions (1×10^7 cells in 0.2 mL culture medium) were injected subcutaneously into the left back of C57BL/6J mice on day 1. Mice received intraperitoneal injections of α-pinene (100 mg/kg) in 1 v/v% DMSO-containing PBS or vehicle every day from 5 days after the EL-4 Luc inoculation. Tumor volume (minor diameter^2 × major axis × 1/2) was measured using a caliper. Mice were injected intraperitoneally with 150 mg/kg D-luciferin (Promega, Madison, WI, USA), and tumor progression and metastasis were evaluated using the IVIS Lumina (PerkinElmer, Waltham, MA, USA) in vivo imaging system. Tumor tissues collected from mice on day 15 were fixed in 4% PFA in PBS. Details of the immunohistochemistry methods are provided in Appendix S1.

FIGURE 3 α-Pinene-induced mitochondrial respiratory dysfunction and reactive oxygen species are involved in apoptosis in EL-4 cells. (A) Quantification of intracellular 2′,7′-dichlorofluorescein (DCF) levels. EL-4 cells were treated with α-pinene 10 μg/mL with or without *N*-acetyl-L-cysteine (NAC) 10 mM for 1 h and then incubated with 2′,7′-dichlorodihydrofluorescein diacetate (DCFH-DA) for 20 min. Representative histogram showing intracellular DCF levels (left). Median fluorescence intensity (MFI) of intracellular DCF (right). (B) Apoptosis assay of EL-4 cells treated with α-pinene 10 μg/mL with or without NAC 10 mM for 6 h. Representative flow cytometry (FCM) plots of apoptosis assay (left) and percentages of apoptotic cells (right). (C) FCM analysis of intracellular γH2AX levels in EL-4 cells treated with α-pinene 10 μg/mL with or without NAC 10 mM for 6 h. Representative histogram showing intracellular γH2AX levels (left). MFI of intracellular γH2AX (right). (D) FCM analysis of mitochondrial membrane potential in EL-4 cells treated with α-pinene 10 μg/mL with or without NAC 10 mM for 24 h. Representative histogram showing intracellular tetramethylrhodamine ethyl ester (TMRE) levels (left) and the percentage of TMRE$^-$ cells (right). (E) Oxygen consumption rate of EL-4 cells treated with α-pinene 10 μg/mL. (F, G) EL-4 cells treated with or without α-pinene 5 μg/mL for 24 h. Cell culture supernatant was collected, and the glucose consumption (F) and lactate production (G) per 1×10^4 cells were measured. (H) Quantification of mitochondrial superoxide levels. EL-4 cells, resuspended with mtSOX Deep Red, were treated with α-pinene 10 μg/mL with or without NAC 10 mM for 1 h. Representative histogram showing mtSOX Deep Red levels (left). MFI of mtSOX Deep Red (right). All data are based on at least three independent experiments. Results are reported as the mean ± SEM. In (E–G), results were compared with those of the control group using two-tailed, independent samples *t*-tests. In (A–D), and (H), data were analyzed using one-way ANOVA. *$p < 0.05$, **$p < 0.01$, ***$p < 0.001$, ****$p < 0.0001$.
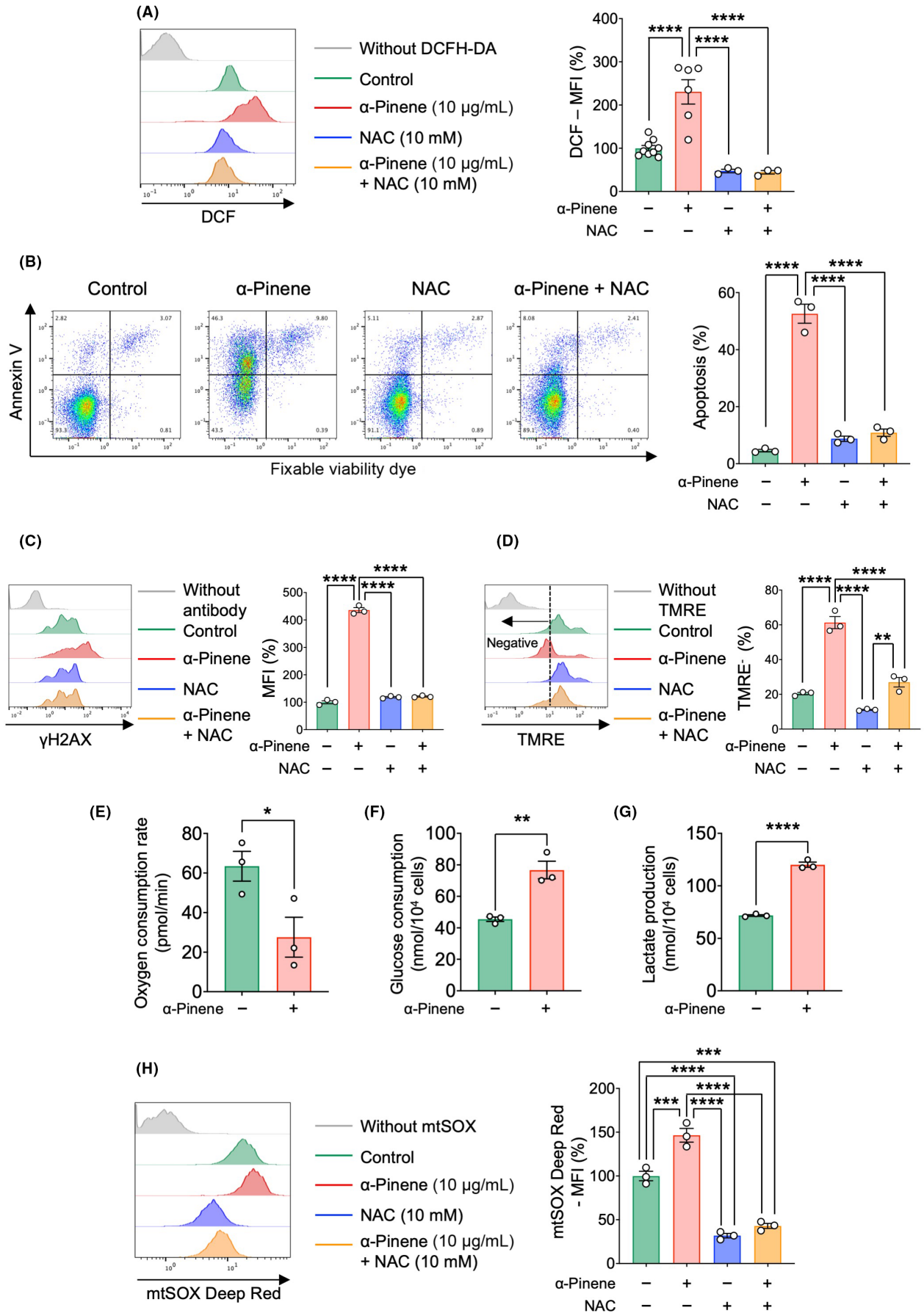
2.18 | Other methods

Detailed descriptions of other methods used in this study are provided in Appendix S1.

2.19 | Statistical analysis

The mean±SEM of at least three independent experiments were reported, unless otherwise specified. Statistical significance was assessed using independent samples t-tests to compare two groups, and one-way ANOVA with a post-hoc test to compare three groups, unless otherwise specified. Statistical analyses were performed using GraphPad Prism 8 (GraphPad Software, San Diego, CA, USA). Two-tailed p-values <0.05 were considered statistically significant.

3 | RESULTS

3.1 | α-Pinene inhibits the proliferation of hematologic malignancies

To examine the antitumor activity of α-pinene on hematologic malignancies, we evaluated the cell growth inhibitory effects of α-pinene for murine and human hematologic malignancy cell lines in vitro. As limonene, another monoterpene present in mastic oil, is reported to have antitumor effects,[6] we included not only α-pinene but also limonene in the experiments to compare the antitumor effects of these monoterpenes. To investigate the efficacy of α-pinene and limonene in hematologic malignancies, we tested these compounds in the T-ALL cell lines, EL-4, Molt-4, CCRF-CEM, and HPB-ALL, the acute myeloid leukemia cell lines, KG-1a and HNT-34, the acute promyelocytic leukemia cell line, HL-60, the chronic myelogenous leukemia cell line, K562, the B-ALL cell lines, BALM-7 and NALM-6, and the multiple myeloma cell line, 5TGM1. α-Pinene was highly effective at inhibiting the growth in EL-4, Molt-4, CCRF-CEM, HPB-ALL, KG-1a, HNT-34, BALM-7, and 5TGM1 (Figure 1A; Figure S1A; Table 1). Among these hematologic malignancies, novel therapies such as B-cell lymphoma 2 (BCL-2) inhibitors, bispecific T-cell engager, and chimeric antigen receptor T-cell therapy have emerged for AML and B-ALL.[12–14] However, given the lack of effective treatments for relapse and refractory T-cell malignancies and considering that the patient population is young, developing a novel agent for T-cell malignancies is imperative. Thus, we focused our investigation on the effect of α-pinene on T-cell tumors. α-Pinene and limonene inhibited the growth of the murine T-cell tumor cell line EL-4 and the human-derived T-cell tumor cell line Molt-4 in vitro in a concentration- and time-dependent manner (Figure 1A,B; Table 1). EL-4 cells incubated with α-pinene or limonene for 36h had an indistinct, necrotic appearance (Figure 1C), whereas limonene had a variable effect. Furthermore, α-pinene and limonene had minimal effect on the growth of human blood T-cells and murine spleen T-cells (Table 1; Figure S1A).

We examined the apoptotic response using Annexin V and fixable viability dye (FVD) staining (Figure S1B). Both α-pinene and limonene triggered apoptosis in EL-4 cells as early as 1h after exposure. Limonene rapidly induced early apoptosis at 2h, but α-pinene induced apoptosis more strongly at 6h (Figure 1D). α-Pinene and limonene also induced apoptosis in Molt-4 cells (Figure S1C). As α-pinene induces cell-cycle arrest in other types of cancers,[15,16] we performed cell-cycle analyses by FCM using Ki67 and DAPI (Figure S1D). Both α-pinene and limonene significantly decreased the proportion of cells in the G1 and M phases, and increased the proportion of cells in the G0 phase (Figure 1E), suggesting that they induced cell-cycle arrest and apoptosis.

3.2 | Transcriptomic profiling of EL-4 and Molt-4 cells treated with α-pinene

We analyzed the transcriptomes of EL-4 and Molt-4 cells treated with α-pinene using RNA-seq to determine the mechanisms underlying the effects of α-pinene. We detected 11,900 genes, including 838 upregulated and 796 downregulated DEGs in EL-4 (Figure 2A–C; Table S2), and 14,614 genes, including 643 upregulated and 288 downregulated DEGs in Molt-4 (Figure S2A–C). GO molecular function analysis revealed enrichment in GO terms related to cellular damage (Figure 2D; Figure S2D; Table S3). Furthermore, biological pathway analyses using KEGG showed that α-pinene treatment enriched genes associated with the ROS pathway and apoptosis (Figure 2E; Figure S2E; Table S4). ROS are primarily generated by mitochondria in most mammalian cells,[17] and mitochondrial DNA

FIGURE 4 α-Pinene stimulates the EGR1-p53-BAX/BCL-2-caspase cascade, leading to apoptosis. Quantitative gene expression analyses of *Egr1* (A) and *Trp53* (B) relative to *Actb* in EL-4 cells treated with α-pinene 10µg/mL at indicative time point. Flow cytometry (FCM) analyses of protein levels of p53 (C) and phosphorylated p53 (D) in EL-4 cells treated with α-pinene 10µg/mL for 3h. (C) Representative histogram showing intracellular p53 levels (left). Median fluorescence intensity (MFI) of intracellular p53 (right). (D) Representative histogram showing intracellular phosphorylated p53 levels (left). MFI of intracellular phosphorylated p53 (right). (E–G) Quantitative gene expression analyses of *Bcl2* (E) and *Bax* (F) relative to *Actb* in EL-4 cells treated with α-pinene 10µg/mL at the specified time point. (G) BAX/BCL-2 ratio. (H) Quantification of active caspase-3 levels. EL-4 cells were treated with α-pinene 10µg/mL with or without *N*-acetyl-L-cysteine (NAC) 10mM for 24h. Representative histogram showing intracellular active caspase-3⁺ levels (left). The percentage of active caspase-3⁺ cells (right). All data are based on at least three independent experiments. Data are reported as the mean±SEM. In (A–G), the results of the experimental and control groups were compared using two-tailed, independent samples t-tests. The data in (H) were analyzed using one-way ANOVA. *$p<0.05$, **$p<0.01$, ***$p<0.001$, ****$p<0.0001$.
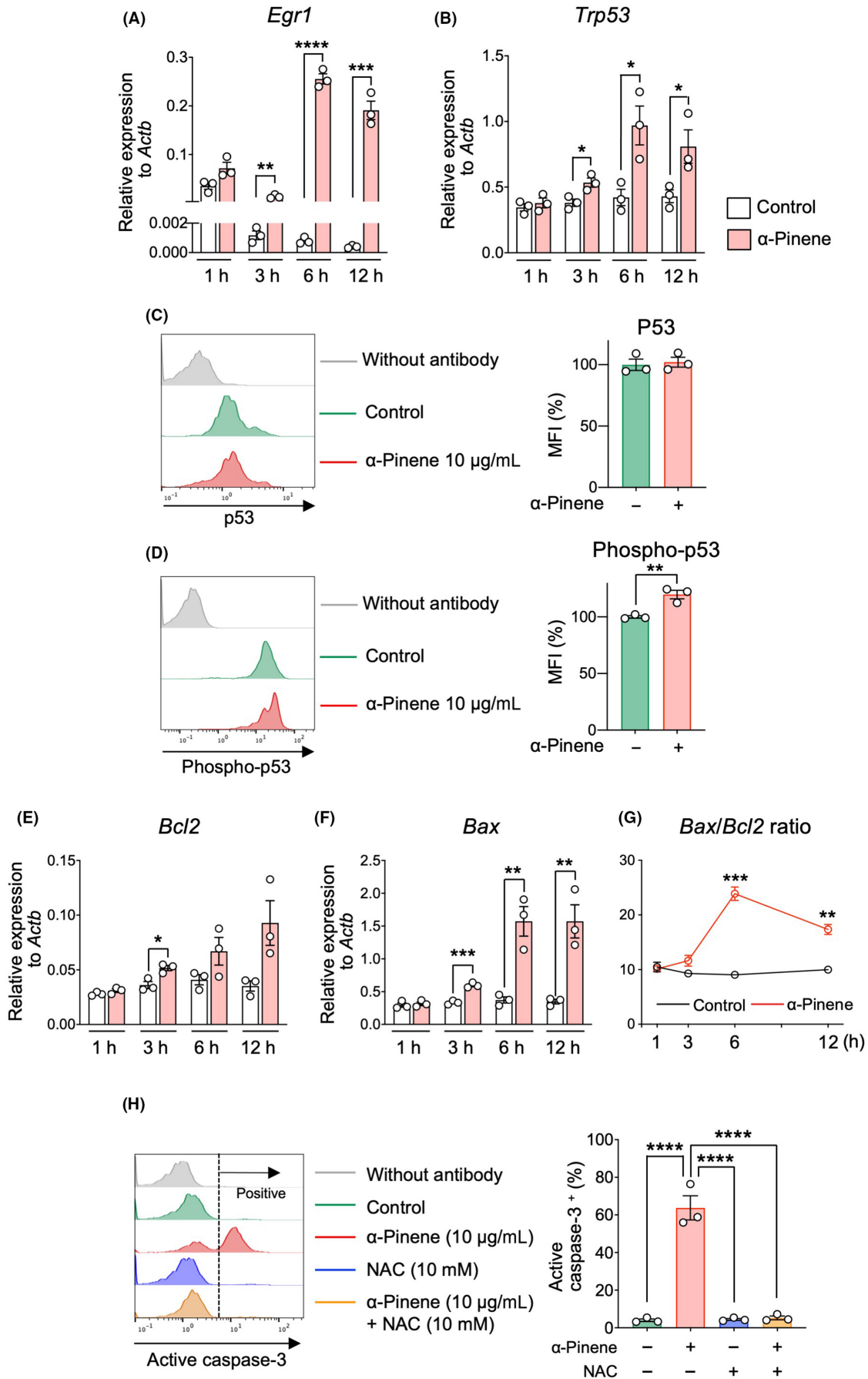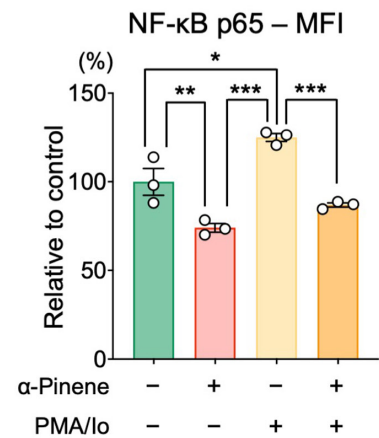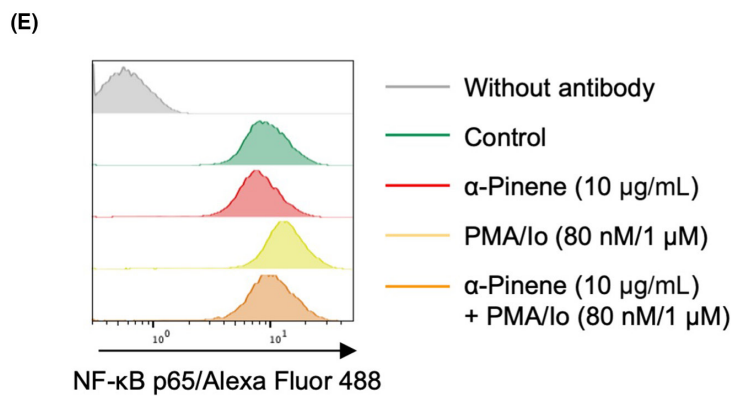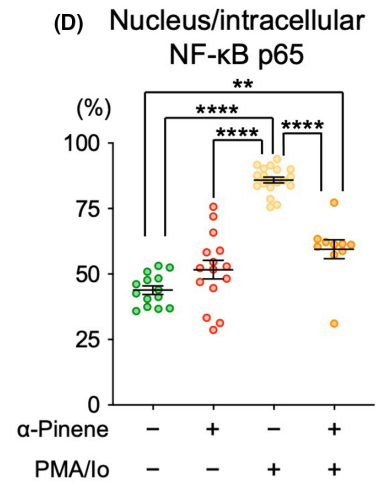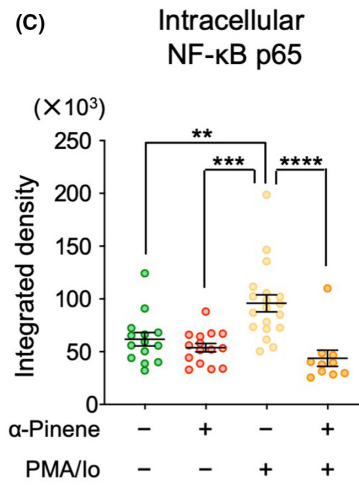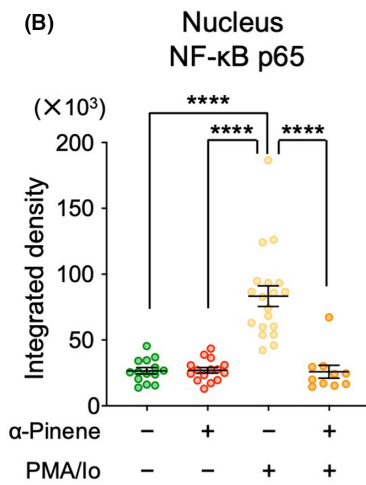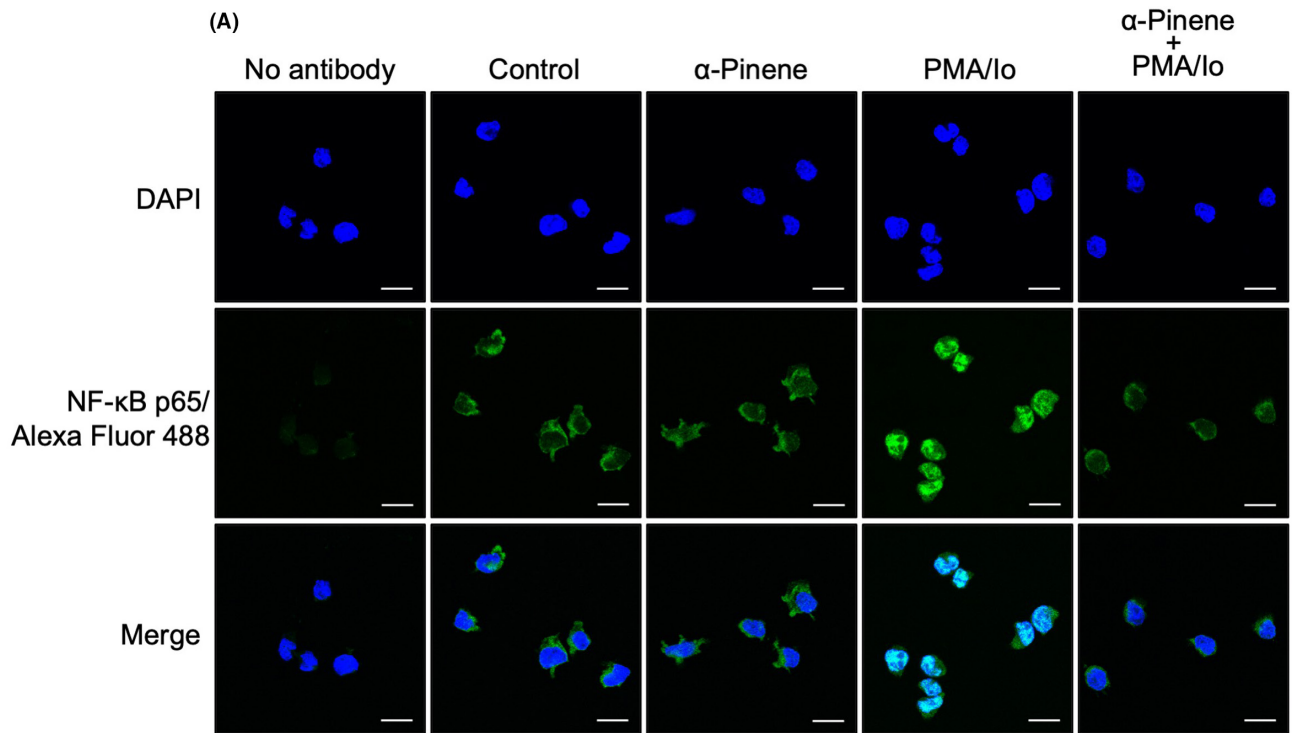
FIGURE 5 α-Pinene reduces total intracellular NF-κB p65 and inhibits NF-κB p65 translocation into the nucleus in EL-4 cells. (A) Representative immunofluorescence imaging showing the location of nuclear factor kappa B (NF-κB) p65 in EL-4 cells. EL-4 cells were treated with α-pinene 10 μg/mL for 4 h and then stimulated with PMA 80 nM and ionomycin (Io) 1 μM (PMA/Io) for 20 min. Alexa Fluor 488-labeled NF-κB p65 in green and DAPI-labeled nucleus in blue. The scale bars show 20 μm. (B–D) Quantification of integrated density of immunofluorescence of Alexa Fluor 488-labeled NF-κB p65 in the nucleus (B) and intracellular (C). (D) Percentage of integrated density of nucleus NF-κB p65 immunofluorescence in the whole cell. (E) Representative histogram showing intracellular Alexa Fluor 488-labeled NF-κB p65 levels in EL-4 cells (left). Median fluorescence intensity (MFI) of intracellular Alexa Fluor 488-labeled NF-κB p65 (right). All data are based on at least three independent experiments. Data are reported as the mean ± SEM. The data were analyzed using one-way ANOVA; *$p < 0.05$, **$p < 0.01$, ***$p < 0.001$, ****$p < 0.0001$.

is more susceptible than nuclear DNA to damage after oxidative stress, leading to mitochondria dysfunction and apoptosis.[18] Thus, we identified GO terms related to mitochondrial dysfunction, including mitochondrial respiration, outer membrane permeability, depolarization and release of cytochrome *c* (Figure 2F; Figure S2F; Table S5). These findings suggest that α-pinene inhibits T-cell tumor proliferation by increasing intracellular ROS levels and inducing mitochondrial dysfunction.

3.3 | α-Pinene induces mitochondrial dysfunction and excessive ROS accumulation in T-cell tumors

Excessive ROS production and mitochondrial damage play crucial roles in inducing apoptosis[19]; therefore, we assessed intracellular ROS levels in EL-4 and Molt-4 cells treated with α-pinene. α-Pinene treatment significantly elevated ROS levels in EL-4 and Molt-4 cells, which was suppressed by co-incubation with the ROS inhibitor, NAC (Figure 3A; Figure S3A). NAC prevented α-pinene-induced apoptosis in EL-4 and Molt-4 cells (Figure 3B; Figure S3B). Because the CCK-8 assay is unreliable in the presence of NAC, we used FCM to count live cells and evaluate the effect of the addition of NAC. NAC almost completely prevented the inhibitory effects of α-pinene on EL-4 and Molt-4 cells (Figure S3C,D), suggesting that the ROS-mediated apoptotic pathway plays a major role in the inhibition of EL-4 and Molt-4 cell growth by α-pinene. As for EL-4 and Molt-4, α-pinene induced the increase in ROS levels and apoptosis induction in CCRF-CEM, HPB-ALL, KG-1a, HNT-34 and BALM-7, indicating that α-pinene might exert an antitumor effect in these cell lines through similar mechanisms (Figure S3E–I).

As α-pinene has been shown to induce DNA damage in malignant melanoma cells,[7] we assessed γH2AX, a biomarker for DNA double-stranded breaks,[20] in EL-4 and Molt-4 cells treated with α-pinene. α-Pinene treatment significantly increased γH2AX both in EL-4 and Molt-4 cells, which was suppressed by co-incubation with NAC (Figure 3C; Figure S4A), suggesting that the increase in ROS preceded DNA damage. Based on the results of RNA-seq (Figure 2F; Figure S2F), we hypothesized a mitochondrial respiratory chain-related dysfunction as the cause of the elevated ROS. First, we assessed the MMP using TMRE. Treatment of α-pinene led to a decrease in MMP in EL-4 and Molt-4 cells, suggesting mitochondrial dysfunction. NAC treatment mitigated the α-pinene-induced reduction in MMP (Figure 3D; Figure S4B). The assessment of

mitochondrial basal OCR in EL-4 showed a decrease after exposure to α-pinene, providing additional evidence of mitochondrial dysfunction (Figure 3E). Next, to examine the impact of impaired mitochondrial respiration, we investigated glucose consumption and lactate production in EL-4 cells treated with α-pinene. α-Pinene treatment increased glucose consumption and lactate production in EL-4 cells (Figure 3F,G), indicating a shift in intracellular energy metabolism from oxidative phosphorylation by mitochondria (OXPHOS) to glycolysis induced by α-pinene. Conversely, in Molt-4 cells, no significant difference in mitochondrial basal OCR was observed following α-pinene treatment (Figure S4C). However, analysis of cell culture supernatant revealed that α-pinene treatment led to an elevation in glucose consumption and lactate production (Figure S4D,E). Furthermore, we examined whether the excessive ROS by α-pinene treatment could increase mitochondrial ROS in EL-4 and Molt-4 cells. As we expected, mitochondrial ROS was increased by α-pinene, which was suppressed by NAC combination (Figure 3H; Figure S4F). These results suggest that α-pinene induces mitochondrial dysfunction that tilts intracellular energy metabolism toward glycolysis and amplifies mitochondrial ROS production in a vicious cycle that ultimately leads to ROS-induced apoptosis and DNA damage.

3.4 | α-Pinene stimulates the EGR1-p53-BAX/ BCL-2-caspase cascade, leading T-cell tumors to apoptosis

RNA-seq analysis revealed that *Egr1/EGR1* gene expression was significantly upregulated in EL-4 and Molt-4 cells treated with α-pinene (Figure 2C; Figure S2C; Table S2), presumably in response to elevated ROS levels. EGR1 is a zinc finger transcription factor that responds to diverse stimuli, including growth factors, cytokines, ROS, hypoxia, and ionizing radiation.[21,22] As EGR1 and ROS target p53,[23,24] a central mediator of cell-cycle arrest and apoptosis, we postulated that the increase in intracellular ROS might result in an elevation of EGR1, consequently activating p53, and subsequently inducing apoptosis. We analyzed the expression of *Egr1* and *Trp53* after α-pinene treatment using a quantitative real-time polymerase chain reaction assay. α-Pinene treatment significantly upregulated the expression of both *Egr1* and *Trp53* in EL-4 cells (Figure 4A,B). Under steady-state conditions, p53 protein is ubiquitinated by MDM2, a negative regulator of p53, and subsequently degraded to maintain low levels.[25] Stress signals phosphorylate human p53 at serine 15, leading to reduced interaction between p53 and MDM2,
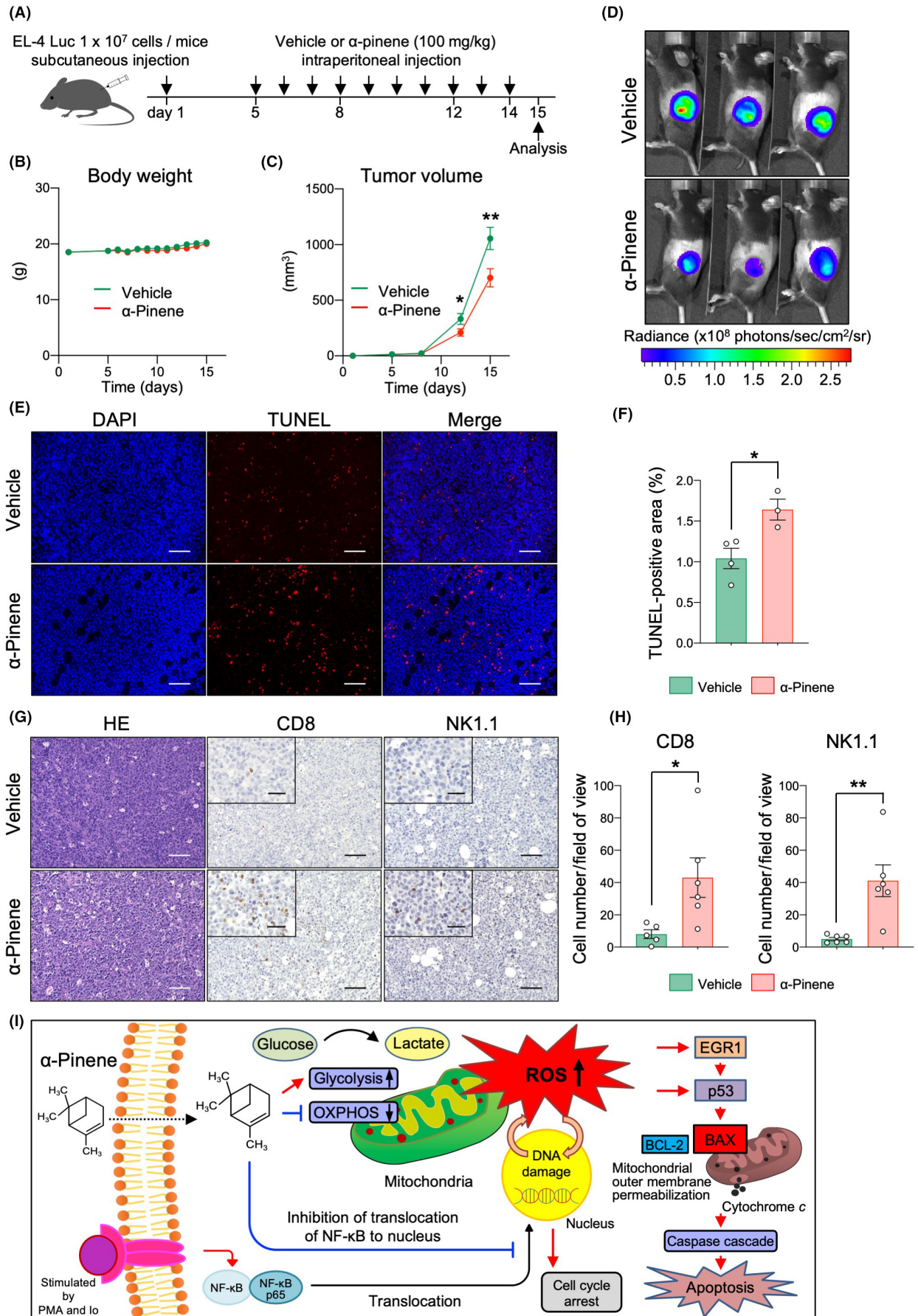
(A) EL-4 Luc 1 x 10⁷ cells / mice subcutaneous injection — Vehicle or α-pinene (100 mg/kg) intraperitoneal injection. day 1, 5, 8, 12, 14, 15 Analysis

(B) Body weight

(C) Tumor volume

(D) Vehicle / α-Pinene — Radiance (x10⁸ photons/sec/cm²/sr)

(E) DAPI / TUNEL / Merge — Vehicle, α-Pinene

(F) TUNEL-positive area (%)

(G) HE / CD8 / NK1.1 — Vehicle, α-Pinene

(H) CD8 / NK1.1 — Cell number/field of view

(I) α-Pinene

FIGURE 6 α-Pinene inhibits EL-4 cell proliferation in vivo. (A) Female C57BL/6J were implanted with EL-4 Luc cells on day 1. Mice received intraperitoneal injection of α-pinene (100 mg/kg) or vehicle every day from days 5 to 14, and analysis was performed on day 15, $n = 19$–23 mice per group, from seven independent experiments. (B) Bodyweight of the mice. (C) The tumor volume was measured twice a week (days 5, 8, 12 and 15). (D) Bioluminescence imaging of EL-4 Luc cells in mice on day 15 imaged by IVIS Lumina. (E–H) Imaging analyses of EL-4 Luc tumors from mice on day 15. (E) Representative images of immunofluorescent staining. Scale bars, 100 μm. (F) TUNEL-positive cell area ratio. (G) Representative images of H&E staining and immunohistochemical staining of CD8 and NK1.1 of the tumor. Scale bars, 100 μm (40 μm in the enlarged images). (H) Analysis of CD8$^+$ (left) and NK1.1$^+$ cells (right). (I) Schematic model of the mechanism of α-pinene-induced cell death in hematologic malignancies. α-Pinene impaired mitochondrial oxidative phosphorylation (OXPHOS) and increased glycolysis capacity. Mitochondrial dysfunction elicits ROS generation, resulting in DNA damage and enhanced expression of EGR1, p53, BAX, and an increased BAX/BCL-2 ratio. As a consequence, DNA damage cause cell-cycle arrest and the elevated ROS levels cause augmented permeability of the mitochondrial outer membrane, leading to cytochrome c release and caspase cascade activation, culminating in apoptosis. Additionally, α-pinene inhibits the activation pathways of the NF-κB. Results are reported as the mean ± SEM. The results were compared with those of the control group using two-tailed, independent samples t-tests. *$p < 0.05$, **$p < 0.01$.

which activates p53.[26] Therefore, we investigated the p53 and phosphorylated p53 levels in EL-4 cells. α-Pinene treatment significantly increased phosphorylated p53 levels (Figure 4C,D) without altering total p53 levels, indicating that α-pinene accelerates phosphorylation of p53 in EL-4 cells.

As p53 regulates the transcriptional activity of BCL-2 family proteins,[27] we examined the gene expression of BCL-2 and BCL-2-associated X protein (BAX), which have opposing effects on apoptosis. Although α-pinene increased the expression of both *Bcl2* and *Bax* in EL-4 (Figure 4E,F), the upregulation of *Bax* was more pronounced, resulting in an increased *Bax/Bcl2* ratio after 6 h (Figure 4G). BAX promotes the loss of MMP, and then cytochrome c is released into the cytosol and activates the caspase cascade, resulting in apoptosis.[28] α-Pinene treatment markedly increased active caspase-3 in EL-4 cells, which was inhibited by NAC treatment (Figure 4H). Next, we analyzed the levels of *TP53* expression after treating Molt-4 cells with α-pinene. Because Molt-4 harbors several mutations in *TP53* that may affect its reactivity to α-pinene,[29] we investigated the *TP53* mutations in previously reported loci, including c.743G>A (p.R248Q), c.331C>G (p.L111V), and c.916C>T (p.R306*) by Sanger sequencing.[30–32] Although these mutations were not detected, a single polymorphism, c.215C>G, which produced the Arg72 variant of p53, was identified in Molt-4 cells (Figure S5A–D), consistent with a previous report.[33] α-Pinene treatment downregulated *EGR1* in Molt-4 cells, but did not alter *TP53* gene expression (Figure S6A,B). α-Pinene treatment increased p53 and phosphorylated p53 levels (Figure S6C,D), leading to significant *BAX* upregulation and an increased *BAX/BCL2* ratio (Figure S6E–G). As in EL-4 cells, the active caspase-3 level was significantly increased in Molt-4 cells treated with α-pinene and this was completely restored by NAC treatment (Figure S6H). These findings suggest that α-pinene inhibits T-cell tumor growth by activating intrinsic apoptotic pathways involving EGR1, p53, BCL-2, BAX, and caspase cascade.

3.5 | α-Pinene inhibits NF-κB p65 translocation into the nucleus and reduces total intracellular NF-κB p65

NF-κB plays a crucial role in regulating various processes in cancer, including cell proliferation, adhesion, and resistance to apoptosis.[34-37]

NF-κB is composed of homo and heterodimers of RelA (p65), RelB, c-Rel, NF-κB1, and NF-κB2. Although inhibitory IκB kinases sequester these protein complexes in the cytoplasm during steady-state conditions, phosphorylation and acetylation lead to their translocation to the nucleus and activation of target-gene transcription.[36,38] Because α-pinene has been reported to inhibit nuclear translocation of NF-κB in the human monocyte cell line THP-1,[39] we examined the impact of α-pinene on the NF-κB pathway in EL-4. In EL-4, NF-κB was present in the cytoplasm in the steady state and after α-pinene treatment, but stimulation with PMA/ionomycin led to its translocation to the nucleus (Figure 5A). We quantified NF-κB translocation by calculating the integrated density of fluorescence bound to NF-κB p65 antibodies in the cytoplasm and nucleus using immunofluorescence staining (Figure 5A–C). The integrated density of NF-κB p65 increased in the cytoplasm and nucleus following PMA/ionomycin treatment (Figure 5A–C), indicating upregulation of NF-κB. The percentage of intracellular NF-κB p65 located in the nucleus increased significantly after PMA/ionomycin stimulation, reflecting PMA/ionomycin-induced nuclear translocation of NF-κB (Figure 5D). α-Pinene inhibited the PMA/ionomycin-induced increase in NF-κB p65 and nuclear translocation (Figure 5A–D). FCM analyses revealed that α-pinene reduced the total amount of intracellular NF-κB p65 and suppressed the increase in NF-κB p65 after stimulation with PMA/ionomycin (Figure 5E), suggesting that α-pinene might inhibit EL-4 proliferation by suppressing the NF-κB pathway.

3.6 | Effect of α-pinene on tumor growth in a mouse T-cell tumor model

To investigate the tumor-suppressive effects of α-pinene in vivo, we administered α-pinene to mice subcutaneously inoculated with EL-4 Luc cells (Figure 6A). α-Pinene did not affect gross appearance, behavior, or body weight, indicating its safety (Figure 6B). Administration of α-pinene suppressed tumor cell growth in immunocompetent C57BL/6J mice (Figure 6C,D). The TUNEL assay revealed an increase in TUNEL-positive apoptotic cells in the α-pinene-treated group (Figure 6E,F). Previous studies have suggested that in mice α-pinene activates antitumor immunity associated with an increase in B-cells, T-cells, and NK cells.[10,11] Thus, we evaluated the immune

cells in the blood, spleen, and bone marrow of mice treated with α-pinene. α-Pinene did not alter the composition of immune cells or hematopoietic stem and progenitors in these organs (Figure S7A–E). However, CD8^{+} T-cells and NK cells were significantly increased in the tumors of mice treated with α-pinene (Figure 6G,H), suggesting that α-pinene may impede tumor proliferation by facilitating immunocyte recruitment within the tumor.

4 | DISCUSSION

These results show that α-pinene has antitumor activity against hematologic malignancies, especially in T-cell tumors. α-Pinene is the low aqueous solubility, and its molecular weight is 136.23 g/mol.[40] Small hydrophobic molecules can penetrate the cell membrane and move into the cell by passive diffusion.[41] In fact, α-pinene was found in the homogenate of astrocytes treated with essential oil containing α-pinene in similar proportions as in the original essential oil.[42] We found that α-pinene induces mitochondrial dysfunction and ROS accumulation, ultimately leading to apoptosis. ROS levels are elevated in cancer cells,[43] promoting pro-tumorigenic signaling and cancer cell proliferation, survival, angiogenesis, and metastasis; however, excessive ROS levels promote anti-tumorigenic signaling and cause irreversible oxidative distress, thereby inducing cancer cell death.[44] Chemotherapeutic agents used to treat leukemia, such as doxorubicin and vincristine, increase ROS levels in leukemic cells.[45,46] Elevated ROS levels in cancer cells augment their sensitivity to anticancer drugs. In ALL, drugs such as artesunate and parthenolide boost intracellular ROS levels and have a synergistic effect with chemotherapeutic agents.[47,48]

The NF-κB signaling pathways play an essential role in the development and progression of cancer.[36] α-Pinene reduces cytoplasmic phosphorylated IκB, IκB kinase, and nuclear NF-κB levels, and inhibits NF-κB-binding activity in macrophages stimulated with lipopolysaccharides.[49] α-Pinene inhibits nuclear translocation of NF-κB p65 in stimulated T-cell tumor cells and decreases intracellular NF-κB p65 protein levels. These results suggest that α-pinene suppresses tumor development and progression by suppressing the response of the NF-κB pathway to various stimuli.

α-Pinene inhibited cell proliferation by inducing apoptosis in various hematologic tumor cell lines. The Molt-4 cells in our experiments harbored a single polymorphism c.215C>G, which produced the Arg72 p53 variant. Compared with the Pro72 variant, the Arg72 p53 variant has stronger transcription-independent apoptosis-inducing activity in the mitochondria.[50] α-Pinene caused a marked loss of MMP in Molt-4. Thus, the mitochondrial transcription-independent apoptosis activation pathway by the Arg72 variant of p53 may be responsible for potent endogenous apoptosis in Molt-4 cells at low levels of α-pinene.

Another mechanism for the antitumor effect of α-pinene is the activation of immune cells. α-Pinene may activate an antitumor immune response, as indicated by an increase in B-cells, T-cells, and NK cells.[10] α-Pinene also enhances antitumor activity by accelerating NK-cell activation and cytotoxicity via the ERK/AKT signaling pathway.[11] Immune checkpoint inhibitors (ICIs) such as programmed death receptor-1 (PD-1) antibodies have revolutionized cancer treatment and are used to treat Hodgkin lymphoma,[51,52] and have antitumor effects on T-cell tumors.[53,54] However, the effect of ICIs is influenced by PD-1 expression in tumor cells, tumor mutation burden, and infiltration of CD8^{+} T-cells into the tumor microenvironment.[55] Most malignant lymphomas have non-inflammatory environments and may eliminate immune cells in the tumor microenvironment due to their high proliferation rate or genetic changes toward immune escape.[54] As our study showed that α-pinene suppressed the proliferation of T-cell tumors and increased CD8^{+} T-cells and NK cells in the tumor, combining α-pinene with ICIs could boost its efficacy in T-cell tumors.

The antitumor effect of α-pinene in the mouse model was not as strong as observed in vitro. This may be because α-pinene is completely eliminated from the human body 10h after exposure, and that α-pinene is highly volatile and may be excreted in the exhaled air,[56] which may explain why α-pinene was not as effective in vivo. This may be the reason why the effect of α-pinene was not high in our mice tumor model. Although α-pinene has limited applications due to its low water solubility, high photosensitivity, and high volatility, attempts have been made to encapsulate α-pinene in solid lipid nanoparticles,[57] cyclodextrins, or liposomes to elicit stable biological effects.[40] It is expected that these technologies will be applied in the future to develop novel drug delivery systems that efficiently deliver α-pinene to tumor cells.

In conclusion, this study showed that α-pinene possesses unique antitumor properties (Figure 6I), which may help in developing novel therapies for hematologic malignancies resistant to conventional chemotherapy. Further investigation of the use of α-pinene for the treatment of hematologic malignancies is warranted.

AUTHOR CONTRIBUTIONS

CONFLICT OF INTEREST STATEMENT

The authors declare no conflict of interest.

ETHICS STATEMENT

Approval of the research protocol by an Institutional Reviewer Board: Human peripheral blood was collected from healthy donors. This study was conducted in accordance with the Declaration of Helsinki and approved by the Okayama University Certified Review Board.

Informed Consent: Written informed consent was obtained from all donors prior to sample collection.

Registry and the Registration No. of the study/trial: N/A.

Animal Studies: All animal experimental procedures were approved by the Animal Care and Use Committee of Okayama University Advanced Science Research Center.

ORCID

Noboru Asada https://orcid.org/0000-0001-7322-5460

REFERENCES

1. Swerdlow SHC E, Harris NL, Jaffe ES, Pileri SA, Stein H, Thiele J. *WHO Classification of Tumours of Haematopoietic & Lymphoid Tissues*. 4th ed. International Agency for Research on Cancer; 2017.
2. Raetz EA, Teachey DT. T-cell acute lymphoblastic leukemia. *Hematology Am Soc Hematol Educ Program*. 2016;2016:580-588. doi:10.1182/asheducation-2016.1.580
3. Moskowitz AJ, Lunning MA, Horwitz SM. How I treat the peripheral T-cell lymphomas. *Blood*. 2014;123:2636-2644. doi:10.1182/blood-2013-12-516245
4. Cordo V, van der Zwet JCG, Cante-Barrett K, Pieters R, Meijerink JPP. T-cell acute lymphoblastic leukemia: a roadmap to targeted therapies. *Blood Cancer Discov*. 2021;2:19-31. doi:10.1158/2643-3230.BCD-20-0093
5. Basholli-Salihu M, Schuster R, Hajdari A, et al. Phytochemical composition, anti-inflammatory activity and cytotoxic effects of essential oils from three Pinus spp. *Pharm Biol*. 2017;55:1553-1560. doi:10.1080/13880209.2017.1309555
6. Spyridopoulou K, Tiptiri-Kourpeti A, Lampri E, et al. Dietary mastic oil extracted from *Pistacia lentiscus* var. chia suppresses tumor growth in experimental colon cancer models. *Sci Rep*. 2017;7:3782. doi:10.1038/s41598-017-03971-8
7. Matsuo AL, Figueiredo CR, Arruda DC, et al. Alpha-Pinene isolated from *Schinus terebinthifolius* Raddi (Anacardiaceae) induces apoptosis and confers antimetastatic protection in a melanoma model. *Biochem Biophys Res Commun*. 2011;411:449-454. doi:10.1016/j.bbrc.2011.06.176
8. Zhao Y, Chen R, Wang Y, Yang Y. Alpha-Pinene inhibits human prostate cancer growth in a mouse xenograft model. *Chemotherapy*. 2018;63:1-7. doi:10.1159/000479863
9. Kusuhara M, Urakami K, Masuda Y, et al. Fragrant environment with alpha-pinene decreases tumor growth in mice. *Biomed Res*. 2012;33:57-61. doi:10.2220/biomedres.33.57
10. Kusuhara M, Maruyama K, Ishii H, et al. A fragrant environment containing alpha-Pinene suppresses tumor growth in mice by modulating the hypothalamus/sympathetic nerve/leptin Axis and immune system. *Integr Cancer Ther*. 2019;18:1534735419845139. doi:10.1177/1534735419845139
11. Jo H, Cha B, Kim H, et al. Alpha-Pinene enhances the anticancer activity of natural killer cells via ERK/AKT pathway. *Int J Mol Sci*. 2021;22:656. doi:10.3390/ijms22020656
12. DiNardo CD, Jonas BA, Pullarkat V, et al. Azacitidine and Venetoclax in previously untreated acute myeloid leukemia. *N Engl J Med*. 2020;383:617-629. doi:10.1056/NEJMoa2012971
13. Kantarjian H, Stein A, Gokbuget N, et al. Blinatumomab versus chemotherapy for advanced acute lymphoblastic leukemia. *N Engl J Med*. 2017;376:836-847. doi:10.1056/NEJMoa1609783
14. Maude SL, Laetsch TW, Buechner J, et al. Tisagenlecleucel in children and young adults with B-cell lymphoblastic leukemia. *N Engl J Med*. 2018;378:439-448. doi:10.1056/NEJMoa1709866
15. Chen W, Liu Y, Li M, et al. Anti-tumor effect of alpha-pinene on human hepatoma cell lines through inducing G2/M cell cycle arrest. *J Pharmacol Sci*. 2015;127:332-338. doi:10.1016/j.jphs.2015.01.008
16. Hou J, Zhang Y, Zhu Y, et al. Alpha-Pinene induces apoptotic cell death via caspase activation in human ovarian cancer cells. *Med Sci Monit*. 2019;25:6631-6638. doi:10.12659/MSM.916419
17. Murphy MP. How mitochondria produce reactive oxygen species. *Biochem J*. 2009;417:1-13. doi:10.1042/BJ20081386
18. Yakes FM, Van Houten B. Mitochondrial DNA damage is more extensive and persists longer than nuclear DNA damage in human cells following oxidative stress. *Proc Natl Acad Sci USA*. 1997;94:514-519. doi:10.1073/pnas.94.2.514
19. Xu Q, Li M, Yang M, et al. Alpha-pinene regulates miR-221 and induces G(2)/M phase cell cycle arrest in human hepatocellular carcinoma cells. *Biosci Rep*. 2018;38:BSR20180980. doi:10.1042/BSR20180980
20. Rogakou EP, Pilch DR, Orr AH, Ivanova VS, Bonner WM. DNA double-stranded breaks induce histone H2AX phosphorylation on serine 139. *J Biol Chem*. 1998;273:5858-5868. doi:10.1074/jbc.273.10.5858
21. Baron V, Adamson ED, Calogero A, Ragona G, Mercola D. The transcription factor Egr1 is a direct regulator of multiple tumor suppressors including TGFbeta1, PTEN, p53, and fibronectin. *Cancer Gene Ther*. 2006;13:115-124. doi:10.1038/sj.cgt.7700896
22. Wang B, Guo H, Yu H, Chen Y, Xu H, Zhao G. The role of the transcription factor EGR1 in cancer. *Front Oncol*. 2021;11:642547. doi:10.3389/fonc.2021.642547
23. Nair P, Muthukkumar S, Sells SF, Han SS, Sukhatme VP, Rangnekar VM. Early growth response-1-dependent apoptosis is mediated by p53. *J Biol Chem*. 1997;272:20131-20138. doi:10.1074/jbc.272.32.20131
24. Krones-Herzig A, Mittal S, Yule K, et al. Early growth response 1 acts as a tumor SuppressorIn vivoandIn vitrovia regulation of p53. *Cancer Res*. 2005;65:5133-5143. doi:10.1158/0008-5472.Can-04-3742
25. Yogosawa S, Yoshida K. Tumor suppressive role for kinases phosphorylating p53 in DNA damage-induced apoptosis. *Cancer Sci*. 2018;109:3376-3382. doi:10.1111/cas.13792
26. Shieh SY, Ikeda M, Taya Y, Prives C. DNA damage-induced phosphorylation of p53 alleviates inhibition by MDM2. *Cell*. 1997;91:325-334. doi:10.1016/s0092-8674(00)80416-x
27. Hemann MT, Lowe SW. The p53-Bcl-2 connection. *Cell Death Differ*. 2006;13:1256-1259. doi:10.1038/sj.cdd.4401962
28. Adams JM, Cory S. The BCL-2 arbiters of apoptosis and their growing role as cancer targets. *Cell Death Differ*. 2018;25:27-36. doi:10.1038/cdd.2017.161

29. Leroy B, Girard L, Hollestelle A, Minna JD, Gazdar AF, Soussi T. Analysis of TP53 mutation status in human cancer cell lines: a reassessment. *Hum Mutat*. 2014;35:756-765. doi:10.1002/humu.22556

30. Rodrigues NR, Rowan A, Smith ME, et al. p53 mutations in colorectal cancer. *Proc Natl Acad Sci USA*. 1990;87:7555-7559. doi:10.1073/pnas.87.19.7555

31. Murai Y, Hayashi S, Takahashi H, Tsuneyama K, Takano Y. Correlation between DNA alterations and p53 and p16 protein expression in cancer cell lines. *Pathol Res Pract*. 2005;201:109-115. doi:10.1016/j.prp.2005.01.002

32. Ikediobi ON, Davies H, Bignell G, et al. Mutation analysis of 24 known cancer genes in the NCI-60 cell line set. *Mol Cancer Ther*. 2006;5:2606-2612. doi:10.1158/1535-7163.MCT-06-0433

33. Ito A, Morita A, Ohya S, Yamamoto S, Enomoto A, Ikekita M. Cycloheximide suppresses radiation-induced apoptosis in MOLT-4 cells with Arg72 variant of p53 through translational inhibition of p53 accumulation. *J Radiat Res*. 2011;52:342-350. doi:10.1269/jrr.10151

34. Krappmann D, Emmerich F, Kordes U, Scharschmidt E, Dorken B, Scheidereit C. Molecular mechanisms of constitutive NF-kappaB/Rel activation in Hodgkin/reed-Sternberg cells. *Oncogene*. 1999;18:943-953. doi:10.1038/sj.onc.1202351

35. Mitsiades N, Mitsiades CS, Poulaki V, et al. Biologic sequelae of nuclear factor-kappaB blockade in multiple myeloma: therapeutic applications. *Blood*. 2002;99:4079-4086. doi:10.1182/blood.v99.11.4079

36. Karin M. Nuclear factor-kappaB in cancer development and progression. *Nature*. 2006;441:431-436. doi:10.1038/nature04870

37. Nagel D, Vincendeau M, Eitelhuber AC, Krappmann D. Mechanisms and consequences of constitutive NF-kappaB activation in B-cell lymphoid malignancies. *Oncogene*. 2014;33:5655-5665. doi:10.1038/onc.2013.565

38. Vallabhapurapu S, Karin M. Regulation and function of NF-kappaB transcription factors in the immune system. *Annu Rev Immunol*. 2009;27:693-733. doi:10.1146/annurev.immunol.021908.132641

39. Zhou JY, Tang FD, Mao GG, Bian RL. Effect of alpha-pinene on nuclear translocation of NF-kappa B in THP-1 cells. *Acta Pharmacol Sin*. 2004;25:480-484.

40. Hammoud Z, Kayouka M, Trifan A, et al. Encapsulation of alpha-Pinene in delivery systems based on liposomes and cyclodextrins. *Molecules*. 2021;26:6840. doi:10.3390/molecules26226840

41. Cooper GM. *The Cell: A Molecular Approach*. 2nd ed. Sinauer Associates; 2000 Transport of small molecules. https://www.ncbi.nlm.nih.gov/books/NBK9847/

42. Elmann A, Mordechay S, Rindner M, Larkov O, Elkabetz M, Ravid U. Protective effects of the essential oil of Salvia fruticosa and its constituents on astrocytic susceptibility to hydrogen peroxide-induced cell death. *J Agric Food Chem*. 2009;57:6636-6641. doi:10.1021/jf901162f

43. Galadari S, Rahman A, Pallichankandy S, Thayyullathil F. Reactive oxygen species and cancer paradox: to promote or to suppress? *Free Radic Biol Med*. 2017;104:144-164. doi:10.1016/j.freeradbiomed.2017.01.004

44. Reczek CR, Chandel NS. The two faces of reactive oxygen species in cancer. *Annu Rev Cancer Biol*. 2017;1:79-98. doi:10.1146/annurev-cancerbio-041916-065808

45. Heaney ML, Gardner JR, Karasavvas N, et al. Vitamin C antagonizes the cytotoxic effects of antineoplastic drugs. *Cancer Res*. 2008;68:8031-8038. doi:10.1158/0008-5472.CAN-08-1490

46. Groninger E, Meeuwsen-De Boer GJ, De Graaf SS, Kamps WA, De Bont ES. Vincristine induced apoptosis in acute lymphoblastic leukaemia cells: a mitochondrial controlled pathway regulated by reactive oxygen species? *Int J Oncol*. 2002;21:1339-1345. doi:10.3892/ijo.21.6.1339

47. Efferth T, Giaisi M, Merling A, Krammer PH, Li-Weber M. Artesunate induces ROS-mediated apoptosis in doxorubicin-resistant T leukemia cells. *PLoS One*. 2007;2:e693. doi:10.1371/journal.pone.0000693

48. Duechler M, Stanczyk M, Czyz M, Stepnik M. Potentiation of arsenic trioxide cytotoxicity by parthenolide and buthionine sulfoximine in murine and human leukemic cells. *Cancer Chemother Pharmacol*. 2008;61:727-737. doi:10.1007/s00280-007-0527-3

49. Kim DS, Lee HJ, Jeon YD, et al. Alpha-Pinene exhibits anti-inflammatory activity through the suppression of MAPKs and the NF-kappaB pathway in mouse peritoneal macrophages. *Am J Chin Med*. 2015;43:731-742. doi:10.1142/S0192415X15500457

50. Dumont P, Leu JI, Della Pietra AC 3rd, George DL, Murphy M. The codon 72 polymorphic variants of p53 have markedly different apoptotic potential. *Nat Genet*. 2003;33:357-365. doi:10.1038/ng1093

51. Younes A, Santoro A, Shipp M, et al. Nivolumab for classical Hodgkin's lymphoma after failure of both autologous stem-cell transplantation and brentuximab vedotin: a multicentre, multicohort, single-arm phase 2 trial. *Lancet Oncol*. 2016;17:1283-1294. doi:10.1016/S1470-2045(16)30167-X

52. Chen R, Zinzani PL, Fanale MA, et al. Phase II study of the efficacy and safety of Pembrolizumab for relapsed/refractory classic Hodgkin lymphoma. *J Clin Oncol*. 2017;35:2125-2132. doi:10.1200/jco.2016.72.1316

53. Khodadoust MS, Rook AH, Porcu P, et al. Pembrolizumab in relapsed and refractory mycosis Fungoides and Sezary syndrome: a multicenter phase II study. *J Clin Oncol*. 2020;38:20-28. doi:10.1200/JCO.19.01056

54. Kline J, Godfrey J, Ansell SM. The immune landscape and response to immune checkpoint blockade therapy in lymphoma. *Blood*. 2020;135:523-533. doi:10.1182/blood.2019000847

55. Topalian SL, Taube JM, Anders RA, Pardoll DM. Mechanism-driven biomarkers to guide immune checkpoint blockade in cancer therapy. *Nat Rev Cancer*. 2016;16:275-287. doi:10.1038/nrc.2016.36

56. Schmidt L, Goen T. Human metabolism of alpha-pinene and metabolite kinetics after oral administration. *Arch Toxicol*. 2017;91:677-687. doi:10.1007/s00204-015-1656-9

57. Zielinska A, Ferreira NR, Durazzo A, et al. Development and optimization of alpha-Pinene-loaded solid lipid nanoparticles (SLN) using experimental factorial design and dispersion analysis. *Molecules*. 2019;24:2683. doi:10.3390/molecules24152683

SUPPORTING INFORMATION

Additional supporting information can be found online in the Supporting Information section at the end of this article.